RESULTS OF RECENT NASA RESEARCH ON LOW-SPEED AERODYNAMIC CHARACTERISTICS OF SUPERSONIC CRUISE AIRCRAFT

Paul L. Coe, Jr.
NASA Langley Research Center

A. B. Graham
Old Dominion University

SUMMARY

The present paper summarizes the results of recent NASA research on the low-speed aerodynamic characteristics of supersonic cruise aircraft. The results indicate that the relatively low values of lift-curve slope produced by highly swept arrow wings, coupled with the low scrape angle of the fuselage, result in relatively low values of take-off and approach lift coefficients. Although acceptable low-speed performance is obtainable for the configurations currently under study, the low-speed deficiencies dictate a design compromise which prohibits such configurations from achieving maximum range potential. However, through the use of more efficient high-lift systems and the application of propulsive-lift concepts, it is possible to optimize the engine-airframe design for maximum range potential and also to provide good low-speed performance. The results also indicate that nose strakes provide significant improvements in directional stability characteristics and that the use of a propulsive lateral control system may provide a solution to problems associated with inherently low levels of lateral control.

INTRODUCTION

The NASA Langley Research Center has initiated a broad research program for the development of a technology base for aircraft capable of cruising efficiently at supersonic speeds. Such configurations typically incorporate a low-aspect-ratio, highly swept arrow wing which has been found to exhibit high levels of aerodynamic efficiency at design Mach numbers of 2.7. (See refs. 1 and 2.) However, these configurations have generally exhibited relatively poor low-speed performance and stability and control characteristics. (See refs. 3 and 4.) The present paper summarizes the results of recent studies conducted to explore means for providing supersonic cruise aircraft with improved low-speed aerodynamic characteristics in the areas of performance, longitudinal stability, lateral-directional stability, and lateral control.

SYMBOLS

C_L	lift coefficient
C_l	rolling-moment coefficient
C_{l_β}	effective dihedral derivative
C_m	pitching-moment coefficient
C_n	yawing-moment coefficient
C_{n_β}	static directional stability derivative
S	wing area
T	engine thrust
W	airplane weight
α	angle of attack
β	angle of sideslip
BLC	boundary-layer control
PLC	propulsive lateral control

LOW-SPEED PERFORMANCE

One of the fundamental considerations in the design of an efficient supersonic cruise vehicle is the sizing of the configuration with regard to wing area and installed thrust requirements. It is recognized that the sizing process involves considerable compromise and that low-speed performance plays a key part in the trade-off.

Presented in figure 1 is an illustration of the classical "thumb print" plot which shows the variation of range with installed thrust-weight ratio (T/W) and wing loading (W/S). From figure 1 it is seen that increased range can generally be obtained by reducing T/W and increasing W/S. However, as shown in figure 2, low-speed operational constraints related to approach speed and take-off field length requirements prohibit the attainment of the maximum range potential. Therefore, improvements in the low-speed performance, which allow the operational requirements to be satisfied with reduced values of T/W and increased values of W/S, will result in increases in range. Figure 3 illustrates the increase in range which has been provided by improved low-speed performance for a configuration currently under study. The NASA generated baseline Advanced Supersonic Technology Concept (designated the AST-100) is predicted to have a range of approximately 7413 km (4000 n. mi.). Improvements in the low-speed performance of this configuration have permitted the low-speed operational requirements to be met with an increased wing loading and a reduced thrust-weight ratio. The resized vehicle (designated the AST-102) is predicted to have a range of approximately 8154 km (4400 n. mi.), which represents an increase of over 10 percent in vehicle range. From figure 3 it is seen that, based on the engine-airframe sizing studies, an additional increase in range of approximately 371 km (200 n. mi.) may be achieved — provided that further improvements in the low-speed performance (which offset the operation constraints) can be obtained. It is, of course, recognized that noise constraints are of critical importance and must also be considered in the final analysis of the engine-airframe sizing studies.

Figure 4 shows the variation of lift coefficient with respect to angle of attack for the baseline configuration in the approach condition. As would be expected, the low-aspect-ratio highly swept arrow wing results in a relatively low value of lift-curve slope, and the low fuselage scrape angle constrains the approach lift coefficient to values of only about 0.6. Furthermore, the relatively high attitude of the configuration, required to obtain the lift coefficient of 0.6, requires the use of a Concorde-type visor nose for improved pilot visibility and also requires an elongated landing-gear installation which results in a weight and volume penalty.

Langley Research Center is currently engaged in research studies intended to evaluate means for providing increased low-speed lift characteristics and thereby minimize or eliminate the low-speed deficiencies. These studies have included the use of propulsive-lift concepts as shown in figure 5. A photograph of a large-scale model of an advanced supersonic technology configuration, which was used to evaluate the propulsive-lift concepts, is shown mounted for tests in the Langley full-scale tunnel in figure 5. The propulsive-lift concepts investigated for improved high-lift performance include (1) the use of boundary-layer control for enhanced flap effectiveness and prevention of flow separation at high flap deflections, (2) the use of upper-surface blowing (USB) for additional circulation lift (this concept also has another advantage in that the trailing-edge flap system may be continuous, rather than the segmented system necessitated by the use of conventional underslung engines), and (3) the use of simple thrust vectoring schemes.

The potential benefits of the propulsive-lift concepts investigated are illustrated in figure 6, which shows the variation of lift coefficient with angle of attack for the concepts studied. The data for the baseline configuration are replotted from figure 4 for comparison. From these data it can be seen that both the thrust vectoring and upper-surface-blowing concepts can provide substantial increases in the low-speed lift capability. For example, both the thrust vectoring and USB concepts are seen to permit a lift coefficient of 0.7 to be obtained at a reduced angle of attack. The increase in lift coefficient (from 0.6 to 0.7) will permit the wing size to be reduced and allow the low-speed operational constraints to be met with an increase in wing loading. This, in turn, may allow the maximum range potential to be realized. Furthermore, the reduced attitude of the configuration may allow for a reduction in landing-gear length and may also eliminate the visor nose requirement, which represents a significant weight savings.

LONGITUDINAL STABILITY

The variation of pitching-moment coefficient with respect to angle of attack for the baseline AST configuration is presented in figure 7. As can be seen from figure 7, the configuration is intended to be flown with a slightly negative static margin (i.e., $\partial C_m/\partial C_L = 0.03$) during the low-speed phases of flight. The impact of the longitudinal instability on the handling qualities of the configuration and the requirements for stability augmentation are discussed in detail in reference 5. The primary concern, however, in the area of longitudinal stability is the nonlinear variation of C_m with α. As shown in figure 7, the basic airframe exhibits a marked nonlinear pitching-moment characteristic for angles of attack greater than about 6°. Results of flow visualization studies have indicated that this nonlinearity is associated with the formation of wing-apex vortices and also with the premature stall of the outboard wing panels. Previous studies of similar configurations have shown that deflection of wing-apex flaps is an effective means of delaying the angle of attack at which these vortices occur. Furthermore, these studies have shown that the use of a Krueger flap on the outboard wing panel is an effective means for providing well attached flow to substantially higher angles of attack. As can be seen from figure 7, when these surfaces are deployed on the current AST concept, the resulting variation of C_m with respect to α is essentially linear. It should be noted that the nonlinearity has a negligible impact on the configuration during normal approach conditions; however, in the gust upset condition, the nonlinearity of the pitching moment would require the longitudinal control surfaces to be sized to provide pitch trim for approximately a 30-percent increase in pitching moment. This would, of course, require a significantly larger control surface, which would penalize the supersonic cruise performance.

LATERAL-DIRECTIONAL STABILITY

Figure 8 presents the variation of the static directional stability derivative C_{n_β} and the effective dihedral derivative C_{l_β} with angle of attack. These data show that in the normal operational angle-of-attack range, the configuration exhibits relatively low values of C_{n_β} and high values of $-C_{l_\beta}$. As discussed in reference 5, this combination of low C_{n_β} and high $-C_{l_\beta}$ results in relatively poor lateral-directional handling qualities. Furthermore, the high level of $-C_{l_\beta}$ is found to require excessive lateral-control capabilities in order to meet established crosswind landing criteria. Therefore, research is currently being conducted in order to obtain increased levels of C_{n_β} and reduced levels of $-C_{l_\beta}$.

It is, of course, recognized that increased directional stability could be provided by increasing the size of the vertical tail; however, this modification would penalize the supersonic cruise performance. Therefore, the use of nose strakes (currently in use on the Concorde) has been investigated. Figure 9 shows the favorable effect of the nose strakes on C_{n_β}. The data indicate large increases in directional stability due to the strakes. For example, at the approach angle of attack of 8°, the strakes approximately double the value of C_{n_β}. It should be noted that the particular nose strakes investigated were simply intended to determine if increased levels of C_{n_β} could be obtained; unfortunately, these strakes also produced a slight pitchup tendency. However, it is considered that with careful attention to strake detail, increased levels of C_{n_β} can be provided without the attendant pitchup characteristics.

In addition to relatively low levels of C_{n_β}, the configuration may also be subject to large out-of-trim moments. Figure 10 shows that the baseline configuration exhibited large asymmetric yawing-moment coefficients at high angles of attack during wind-tunnel tests of several models. Previous studies conducted at Langley (see, for example, ref. 6) have shown that these asymmetric yawing moments are due to the formation of asymmetrically disposed vortices on long slender fuselage forebodies. For the present configuration the significance of these asymmetries is particularly critical in that at high angles of attack, the magnitude of the yawing moment produced at $\beta = 0^\circ$ is found to be in excess of the directional control power. (See fig. 10.) Such asymmetries are probably sensitive to Reynolds number; however, reference 7 indicates that this phenomenon may persist at Reynolds numbers corresponding to those of the full-scale aircraft. As shown in figure 10, the use of the previously discussed nose strakes is an effective means for eliminating these asymmetric yawing moments.

Previous investigations (see ref. 8) have indicated that reductions in $-C_{l_\beta}$ may be obtained by increasing the load on the inboard portion of the wing. Figure 11 shows the variation of C_L with α and the corresponding variation of C_{l_β} with C_L for two trailing-edge flap deflections. As expected, increasing the trailing-edge flap deflection from 0° provides an increase in lift coefficient at a given angle of attack and also provides a substantial reduction in $-C_{l_\beta}$ at a given lift coefficient. Additional results obtained for this configuration indicate that the reduction in $-C_{l_\beta}$ is primarily associated with the reduction in angle of attack at which the given lift coefficient was obtained and that the level of C_{l_β} appears to be essentially independent of the spanwise variation of the deflection of the trailing-edge flap segments. Although further study is required to validate this conclusion, the data of figure 11 indicate that if further reductions in the operational angle of attack can be obtained (for example with the use of propulsive-lift concepts), it may be possible to provide further reductions in $-C_{l_\beta}$.

LATERAL CONTROL

As mentioned previously, the high levels of effective dihedral produced by highly swept arrow wings require an excessive amount of lateral control power in order to satisfy established crosswind landing criteria. Figure 12 illustrates the severity of the problem for the baseline configuration. The solid curve presented in figure 12 is the amount of lateral control required in order to obtain lateral trim with 10° of sideslip. The dashed curve of figure 12 is the amount of lateral control currently available for the configuration. The significant point brought out by the data of figure 12 is that at the normal approach condition the amount of lateral control required for the NASA baseline configuration is significantly in excess of the control currently available.

In light of these considerations Langley is exploring means for providing increased lateral control capabilities. One promising concept employs propulsive lateral control (PLC) nozzles as shown in figure 13. With the propulsive lateral control system, a portion of the nozzle exhaust flow is vented over the trailing-edge flap during the low-speed phases of flight. Recent studies have shown that this arrangement provides levels of additional circulation lift which are comparable with the USB concept. In addition, the arrangement allows increased lateral control to be obtained by management of the additional circulation lift. This increase in control is accomplished by rotating the slider block system shown in the sketch of figure 13. With the slider block in the closed position, the exhaust flow is prevented from flowing over the trailing-edge flap segments, and hence, additional circulation lift is not generated on the appropriate wing panels. Recent studies indicate that this arrangement will provide approximately a 25-percent increase in roll control. It should be noted that even greater increases in roll control can be provided by combining differential thrust vectoring with the PLC concept.

The impact of the increased lift and increased roll control capability provided by the propulsive lateral control nozzle concept is illustrated in figure 14. As can be seen in figure 14, the increase in lift from this concept permits a reduction in angle of attack for the approach condition, which, when coupled with the increase in lateral control, provides the configuration with sufficient lateral control to meet the crosswind landing criteria at the design approach lift coefficient.

CONCLUDING REMARKS

The results of recent research on the low-speed aerodynamic characteristics of supersonic cruise aircraft indicate that improved low-speed performance can be achieved with more efficient high-lift systems and the application of propulsive-lift concepts. The improved low-speed performance allows the configuration to be configured so as to achieve its maximum range potential. The results also indicate that significant improvements can be obtained in the lateral-directional characteristics with the use of nose strakes and by the introduction of propulsive lateral control concepts.

REFERENCES

1. Morris, Odell A.; and Fournier, Roger H.: Aerodynamic Characteristics at Mach Numbers 2.30, 2.60 and 2.96 of a Supersonic Transport Model Having A Fixed, Warped Wing. NASA TM X-1115, 1965.

2. Morris, Odell A.; and Patterson, James C., Jr.: Transonic Aerodynamic Characteristics of a Supersonic Transport Model With A Fixed, Warped Wing Having 74° Sweep. NASA TM X-1167, 1965.

3. Shivers, James P.; McLemore, H. Clyde; and Coe, Paul L., Jr.: Low-Speed Wind Tunnel Investigation of a Large-Scale Advanced Arrow Wing Supersonic Transport Configuration with Engines Mounted Above the Wing for Upper-Surface Blowing. NASA TM X-72761, 1975.

4. Coe, Paul L., Jr.; McLemore, H. Clyde; and Shivers, James P.: Effects of Upper-Surface Blowing and Thrust Vectoring on Low-Speed Aerodynamic Characteristics of a Large-Scale Supersonic Transport Model. NASA TM X-72792, 1975.

5. Grantham, William D.; Nguyen, Luat T.; Neubauer, M. J., Jr.; and Smith, Paul M.: Simulator Study of the Low-Speed Handling Qualities of a Supersonic Cruise Arrow-Wing Configuration During Approach and Landing. SCAR Conference, Hampton, VA, Nov. 1976, pp. 100-120. (Paper no. 11 of this compilation.)

6. Coe, Paul L., Jr.; Chambers, Joseph R.; and Letko, William: Asymmetric Lateral-Directional Characteristics of Pointed Bodies of Revolution at High Angles of Attack. NASA TN D-7095, 1972.

7. Chapman, Gary T.; Keener, Earl R.; and Malcolm, Gerald N.: Asymmetric Aerodynamic Forces on Aircraft Forebodies at High Angles of Attack — Some Design Guides. Stall/Spin Problems of Military Aircraft, AGARD-CP-199, June 1976, paper no. 12.

8. Lockwood, Vernard E.: Effect of Trailing Edge Flap Deflection on the Lateral and Longitudinal-Stability Characteristics of a Supersonic Transport Model Having a Highly-Swept Arrow Wing. NASA TM X-71936, 1974.

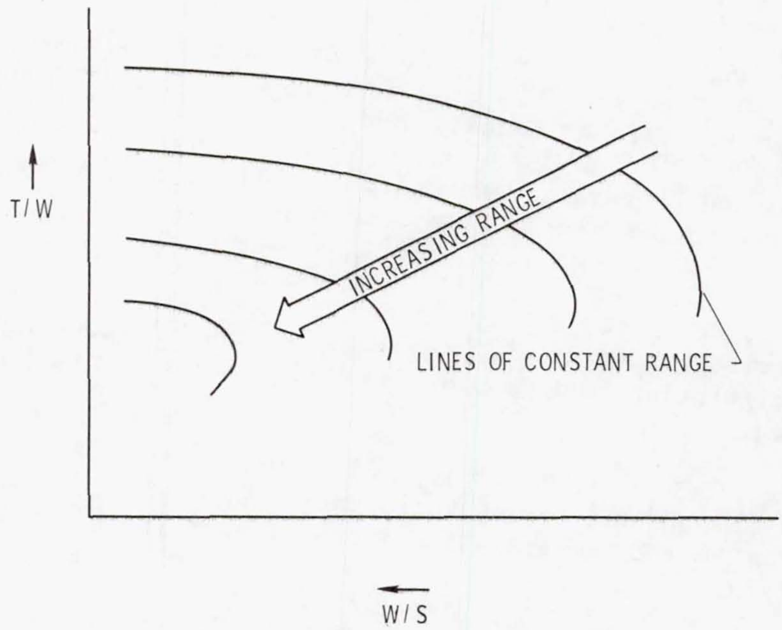

Figure 1.- Variation of range with T/W and W/S.

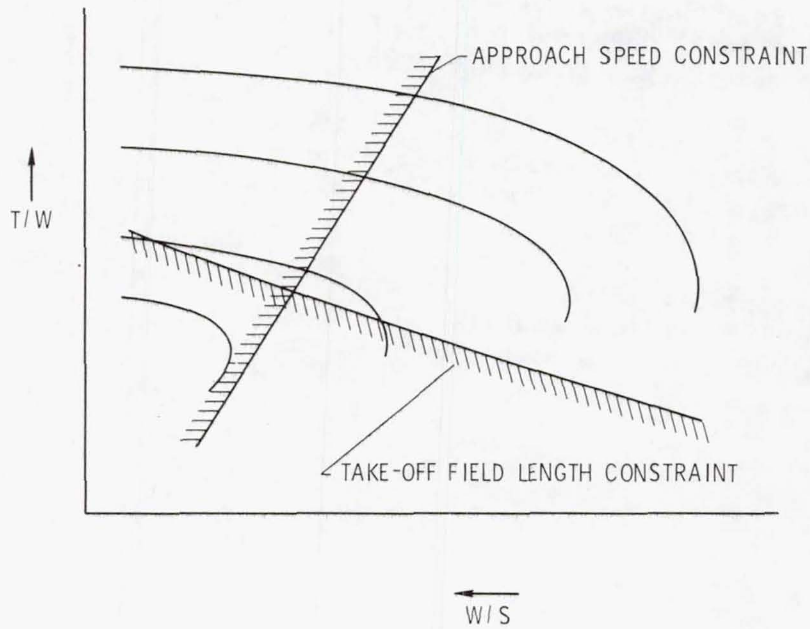

Figure 2.- Low-speed operational constraints.

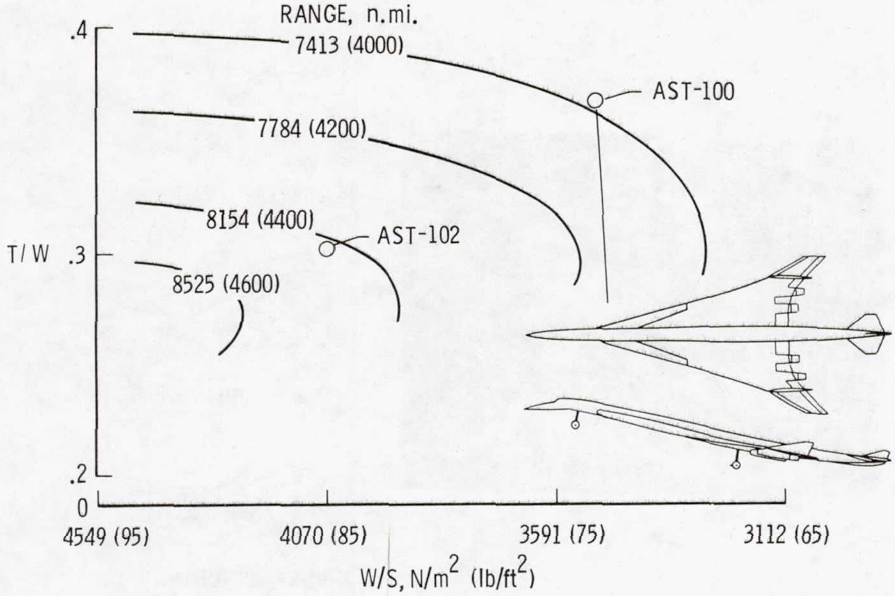

Figure 3.- Increased range provided by improved low-speed performance.

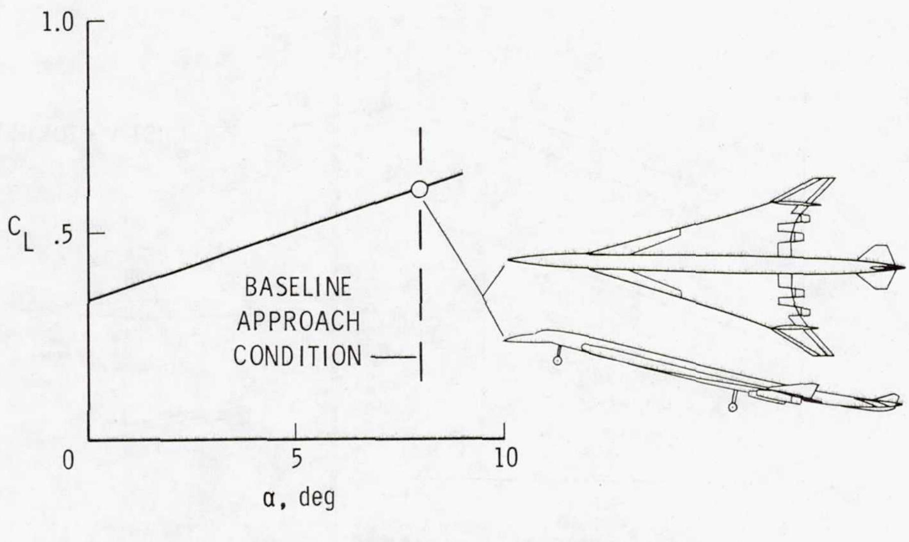

Figure 4.- Variation of C_L with α.

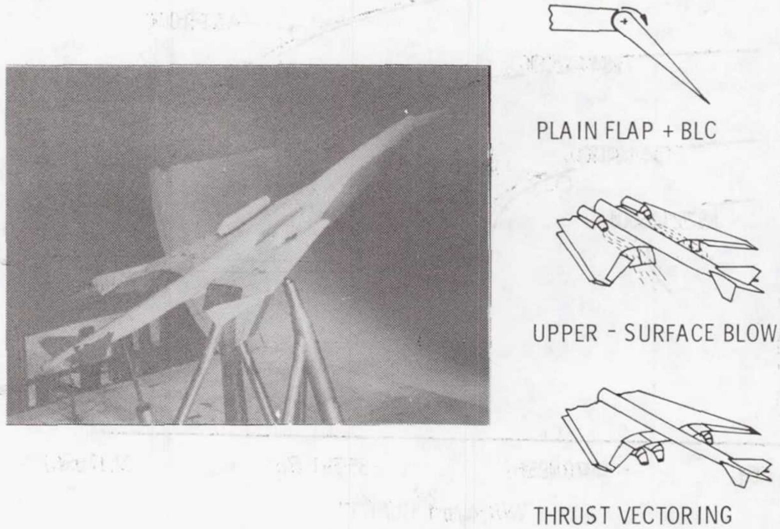

Figure 5.- Propulsive-lift concepts investigated.

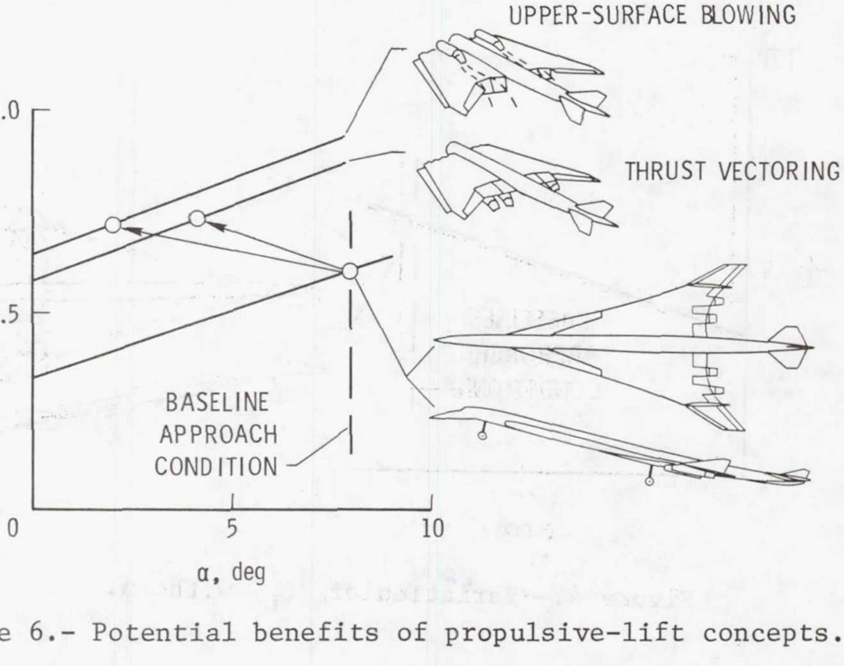

Figure 6.- Potential benefits of propulsive-lift concepts.

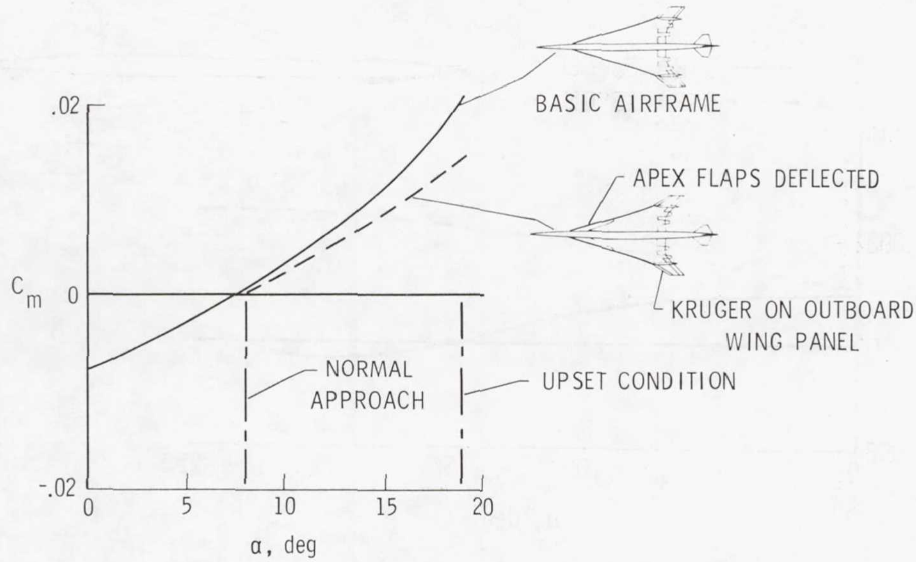

Figure 7.- Variation of C_m with α.

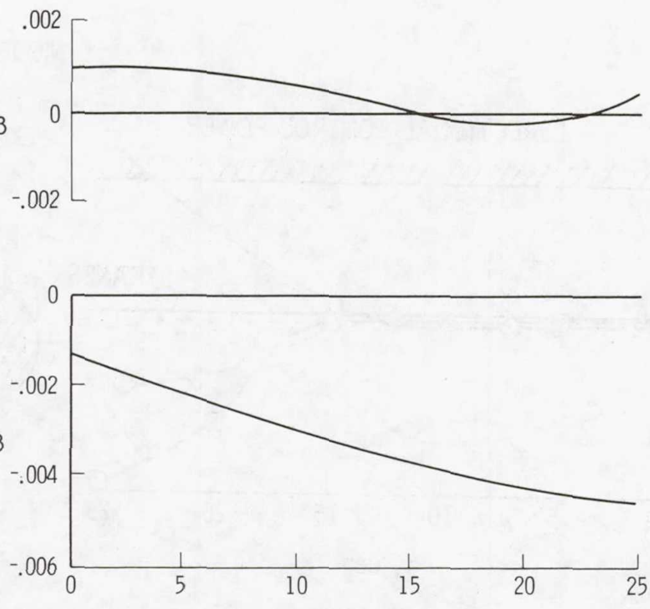

Figure 8.- Static lateral-directional stability characteristics.

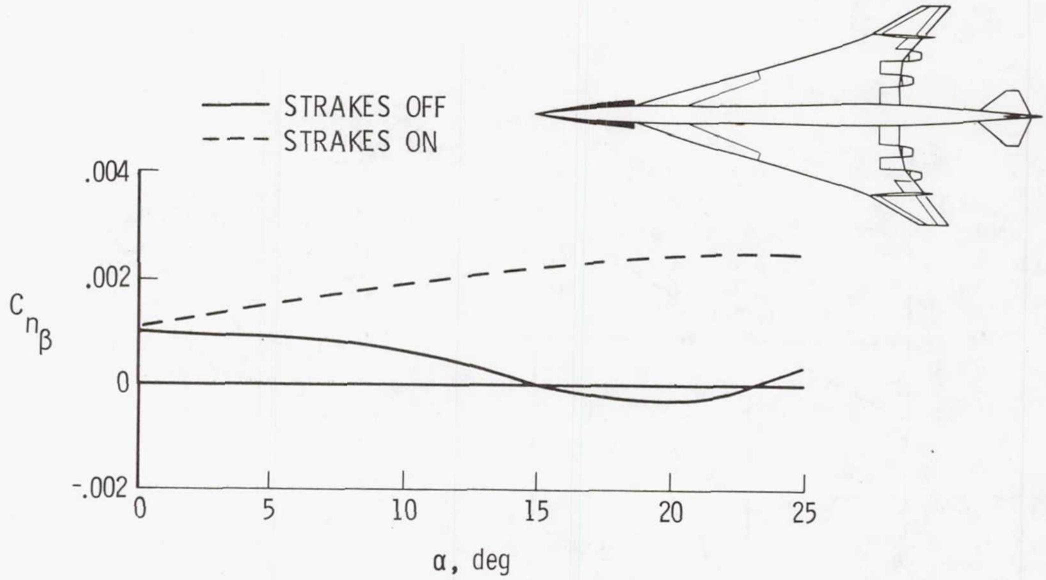

Figure 9.- Effect of nose strakes on C_{n_β}.

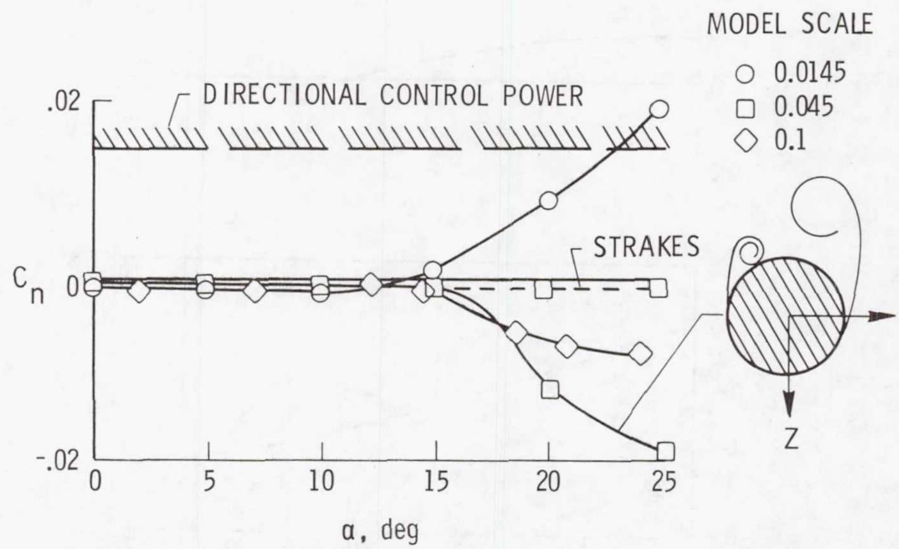

Figure 10.- Forebody-induced asymmetric yawing-moment coefficient. $\beta = 0^o$.

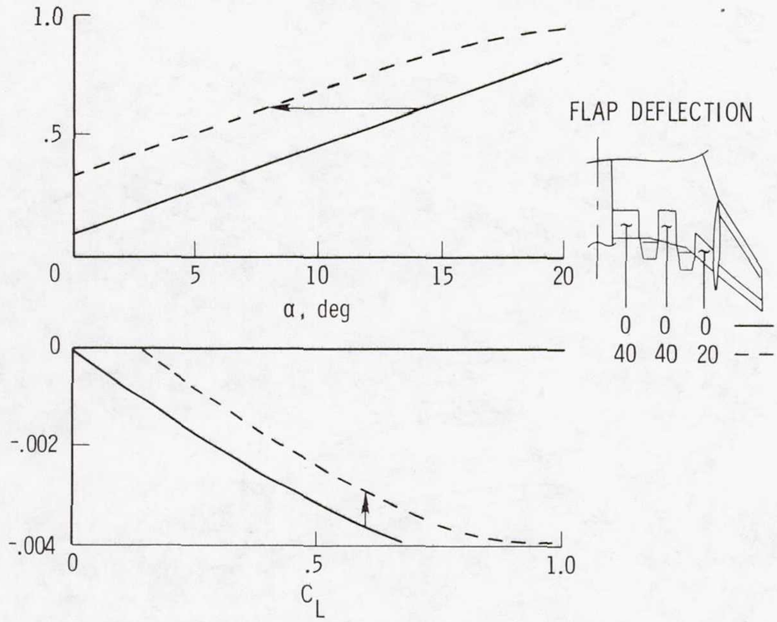

Figure 11.- Variation of C_{l_β} with C_L.

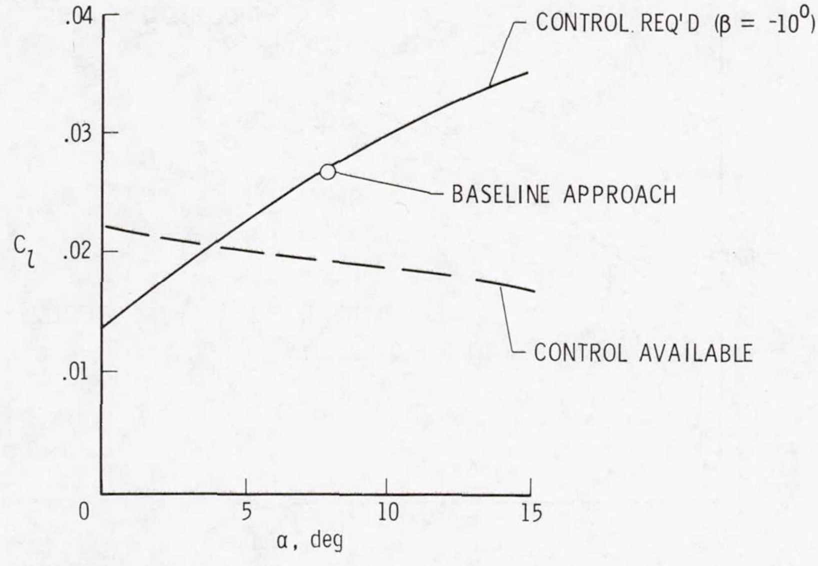

Figure 12.- Lateral control requirements for crosswind landing.

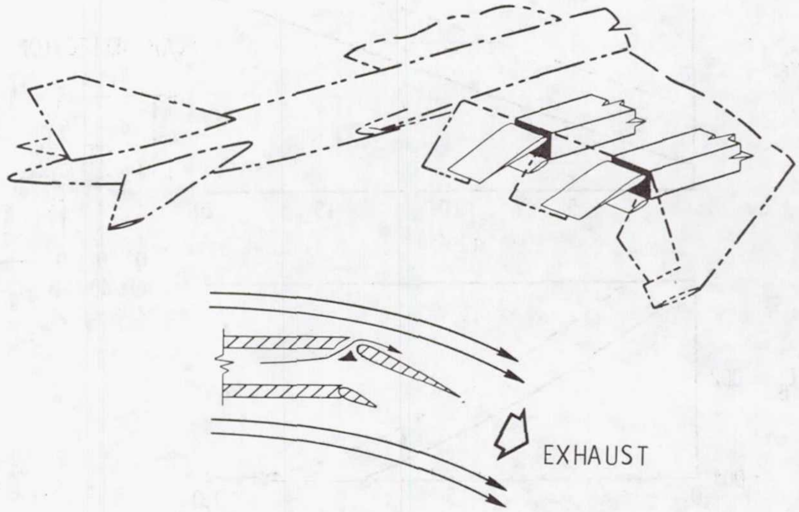

Figure 13.- Sketch of propulsive lateral control nozzle.

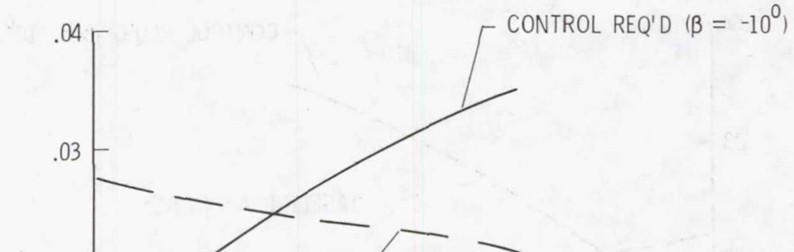

Figure 14.- Lateral control requirements for configuration with propulsive lateral control nozzles.